



Original citation:

LHCb Collaboration (Including: Back, J. J., Blake, T., Craik, Daniel, Dossett, D., Gershon, T. J., Kreps, Michal, Latham, Thomas, Pilar, T., Poluektov, Anton, Reid, Matthew M., Silva Coutinho, R., Wallace, Charlotte, Whitehead, M. (Mark) and Williams, M. P.). (2014) Observation of photon polarization in the $b \rightarrow s\gamma$ transition. *Physical Review Letters*, Volume 112 (Number 16). Article number 161801.

Permanent WRAP url:

<http://wrap.warwick.ac.uk/62998>

Copyright and reuse:

The Warwick Research Archive Portal (WRAP) makes this work of researchers of the University of Warwick available open access under the following conditions.

This article is made available under the Creative Commons Attribution- 3.0 Unported (CC BY 3.0) license and may be reused according to the conditions of the license. For more details see <http://creativecommons.org/licenses/by/3.0/>

A note on versions:

The version presented in WRAP is the published version, or, version of record, and may be cited as it appears here.

For more information, please contact the WRAP Team at: publications@warwick.ac.uk

warwick**publications**wrap

highlight your research

<http://wrap.warwick.ac.uk/>



Observation of Photon Polarization in the $b \rightarrow s\gamma$ Transition

R. Aaij *et al.*^{*}

(LHCb Collaboration)

(Received 27 February 2014; published 22 April 2014)

This Letter presents a study of the flavor-changing neutral current radiative $B^\pm \rightarrow K^\pm \pi^\mp \pi^\pm \gamma$ decays performed using data collected in proton-proton collisions with the LHCb detector at 7 and 8 TeV center-of-mass energies. In this sample, corresponding to an integrated luminosity of 3 fb^{-1} , nearly 14 000 signal events are reconstructed and selected, containing all possible intermediate resonances with a $K^\pm \pi^\mp \pi^\pm$ final state in the $[1.1, 1.9] \text{ GeV}/c^2$ mass range. The distribution of the angle of the photon direction with respect to the plane defined by the final-state hadrons in their rest frame is studied in intervals of $K^\pm \pi^\mp \pi^\pm$ mass and the asymmetry between the number of signal events found on each side of the plane is obtained. The first direct observation of the photon polarization in the $b \rightarrow s\gamma$ transition is reported with a significance of 5.2σ .

DOI: 10.1103/PhysRevLett.112.161801

PACS numbers: 13.20.He, 12.15.Mm, 14.40.Nd

The standard model (SM) predicts that the photon emitted from the electroweak penguin loop in $b \rightarrow s\gamma$ transitions is predominantly left-handed, since the recoiling s quark that couples to a W boson is left-handed. This implies maximal parity violation up to small corrections of the order m_s/m_b . While the measured inclusive $b \rightarrow s\gamma$ rate [1] agrees with the SM calculations, no direct evidence exists for a nonzero photon polarization in this type of decay. Several extensions of the SM [2], compatible with all current measurements, predict that the photon acquires a significant right-handed component, in particular, due to the exchange of a heavy fermion in the penguin loop [3].

This Letter presents a study of the radiative decay $B^+ \rightarrow K^+ \pi^- \pi^+ \gamma$, previously observed at the B factories with a measured branching fraction of $(27.6 \pm 2.2) \times 10^{-6}$ [1,4,5]. The inclusion of charge-conjugate processes is implied throughout. Information about the photon polarization is obtained from the angular distribution of the photon direction with respect to the normal to the plane defined by the momenta of the three final-state hadrons in their center-of-mass frame. The shape of this distribution, including the *up-down asymmetry* between the number of events with the photon on either side of the plane, is determined. This investigation is conceptually similar to the historical experiment that discovered parity violation by measuring the up-down asymmetry of the direction of a particle emitted in a weak decay with respect to an axial vector [6]. In $B^+ \rightarrow K^+ \pi^- \pi^+ \gamma$ decays, the up-down asymmetry is proportional to the photon polarization λ_γ [7,8] and therefore measuring a value different from zero corresponds to demonstrating that the photon is polarized. The

currently limited knowledge of the structure of the $K^+ \pi^- \pi^+$ mass spectrum, which includes interfering kaon resonances, prevents the translation of a measured asymmetry into an actual value for λ_γ .

The differential $B^+ \rightarrow K^+ \pi^- \pi^+ \gamma$ decay rate can be described in terms of θ , defined in the rest frame of the final state hadrons as the angle between the direction opposite to the photon momentum \vec{p}_γ and the normal $\vec{p}_{\pi,\text{slow}} \times \vec{p}_{\pi,\text{fast}}$ to the $K^+ \pi^- \pi^+$ plane, where $\vec{p}_{\pi,\text{slow}}$ and $\vec{p}_{\pi,\text{fast}}$ correspond to the momenta of the lower and higher momentum pions, respectively. Following the notation and developments of Ref. [7], the differential decay rate of $B^+ \rightarrow K^+ \pi^- \pi^+ \gamma$ can be written as a fourth-order polynomial in $\cos \theta$

$$\frac{d\Gamma}{ds ds_{13} ds_{23} d\cos \theta} \propto \sum_{i=0,2,4} a_i(s, s_{13}, s_{23}) \cos^i \theta + \lambda_\gamma \sum_{j=1,3} a_j(s, s_{13}, s_{23}) \cos^j \theta, \quad (1)$$

where $s_{ij} = (p_i + p_j)^2$ and $s = (p_1 + p_2 + p_3)^2$, and p_1 , p_2 , and p_3 are the four-momenta of the π^- , π^+ , and K^+ mesons, respectively. The functions a_k depend on the resonances present in the $K^+ \pi^- \pi^+$ mass range of interest and their interferences. The up-down asymmetry is defined as

$$\mathcal{A}_{\text{ud}} \equiv \frac{\int_0^1 d\cos \theta \frac{d\Gamma}{d\cos \theta} - \int_{-1}^0 d\cos \theta \frac{d\Gamma}{d\cos \theta}}{\int_{-1}^1 d\cos \theta \frac{d\Gamma}{d\cos \theta}}, \quad (2)$$

which is proportional to λ_γ .

The LHCb detector [9] is a single-arm forward spectrometer covering the pseudorapidity range $2 < \eta < 5$, designed for the study of particles containing b or c quarks. The detector includes a high-precision tracking system consisting of a silicon-strip vertex detector surrounding the

*Full author list given at the end of the article.

pp interaction region, a large-area silicon-strip detector located upstream of a dipole magnet with a bending power of about 4 Tm, and three stations of silicon-strip detectors and straw drift tubes placed downstream. The combined tracking system provides a momentum measurement with relative uncertainty that varies from 0.4% at 5 GeV/c to 0.6% at 100 GeV/c , and impact parameter resolution of 20 μm for tracks with a few GeV/c of transverse momentum (p_T). Different types of charged hadrons are distinguished by information from two ring-imaging Cherenkov detectors. Photon, electron, and hadron candidates are identified by a calorimeter system consisting of scintillating-pad and preshower detectors, an electromagnetic calorimeter, and a hadronic calorimeter. The trigger consists of a hardware stage, based on information from the calorimeter and muon systems, followed by a software stage, which applies a full event reconstruction.

Samples of simulated events are used to understand signal and backgrounds. In the simulation, pp collisions are generated using PYTHIA [10] with a specific LHCb configuration [11]. Decays of hadronic particles are described by EVTGEN [12], in which final state radiation is generated using PHOTOS [13]. The interaction of the generated particles with the detector and its response are implemented using the GEANT4 toolkit [14] as described in Ref. [15].

This analysis is based on the LHCb data sample collected from pp collisions at 7 and 8 TeV center-of-mass energies in 2011 and 2012, respectively, corresponding to 3 fb^{-1} of integrated luminosity. The $B^+ \rightarrow K^+\pi^-\pi^+\gamma$ candidates are built from a photon candidate and a hadronic system reconstructed from a kaon and two oppositely charged pions satisfying particle identification requirements. Each of the hadrons is required to have a minimum p_T of 0.5 GeV/c and at least one of them needs to have a p_T larger than 1.2 GeV/c . The isolation of the $K^+\pi^-\pi^+$ vertex from other tracks in the event is ensured by requiring that the χ^2 of the three-track vertex fit and the χ^2 of all possible vertices that can be obtained by adding an extra track differ by more than 2. The $K^+\pi^-\pi^+$ mass is required to be in the [1.1, 1.9] GeV/c^2 range. High transverse energy (> 3.0 GeV) photon candidates are constructed from energy depositions in the electromagnetic calorimeter. The absence of tracks pointing to the calorimeter is used to distinguish neutral from charged electromagnetic particles. A multivariate algorithm based on the energy cluster shape parameters is used to reject approximately 65% of the $\pi^0 \rightarrow \gamma\gamma$ background in which the two photons are reconstructed as a single cluster, while keeping about 95% of the signal photons. The B^+ candidate mass is required to be in the [4.3, 6.9] GeV/c^2 range. Backgrounds that are expected to peak in this mass range are suppressed by removing all candidates consistent with a $D^0 \rightarrow K^+\pi^-\pi^0$ or $\rho^+ \rightarrow \pi^+\pi^0$ decay when the photon candidate is assumed to be a π^0 .

A boosted decision tree [16,17] is used to further improve the separation between signal and background. Its training is based on the following variables: the impact parameter χ^2 of the B^+ meson and of each of the final state hadrons, defined as the difference between the χ^2 of a primary vertex (PV) reconstructed with and without the considered particle; the cosine of the angle between the reconstructed B^+ momentum and the vector pointing from the PV to the B^+ decay vertex; the flight distance of the B^+ meson, and the $K^+\pi^-\pi^+$ vertex χ^2 .

The mass distribution of the selected $B^+ \rightarrow K^+\pi^-\pi^+\gamma$ signal is modeled with a double-tailed Crystal Ball [18] probability density function (PDF), with power-law tails above and below the B mass. The four tail parameters are fixed from simulation; the width of the signal peak is fit separately for the 2011 and 2012 data to account for differences in calorimeter calibration. Combinatorial and partially reconstructed backgrounds are considered in the fit, the former modeled with an exponential PDF, the latter described using an ARGUS PDF [19] convolved with a Gaussian function with the same width as the signal to account for the photon energy resolution. The contribution to the partially reconstructed background from events with only one missing pion is considered separately.

The fit of the mass distribution of the selected $B^+ \rightarrow K^+\pi^-\pi^+\gamma$ candidates (Fig. 1) returns a total signal yield of 13876 ± 153 events, the largest sample recorded for this channel to date. Figure 2 shows the background-subtracted $K^+\pi^-\pi^+$ mass spectrum determined using the technique of Ref. [20], after constraining the B mass to its nominal value. No peak other than that of the $K_1(1270)^+$ resonance can be clearly identified. Many kaon resonances, with various masses, spins, and angular momenta, are expected to contribute and interfere in the considered mass range [1].

The contributions from single resonances cannot be isolated because of the complicated structure of the

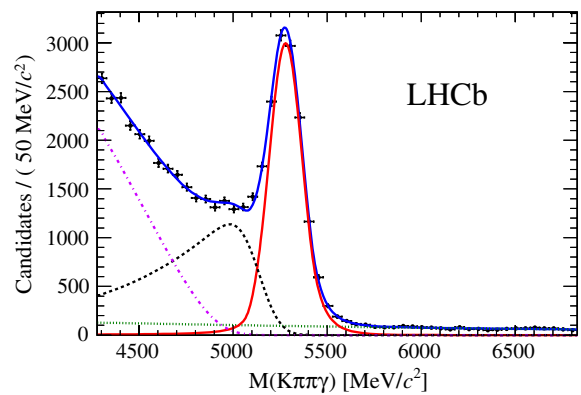


FIG. 1 (color online). Mass distribution of the selected $B^+ \rightarrow K^+\pi^-\pi^+\gamma$ candidates. The blue solid curve shows the fit results as the sum of the following components: signal (red solid), combinatorial background (green dotted), missing pion background (black dashed), and other partially reconstructed backgrounds (purple dash-dotted).

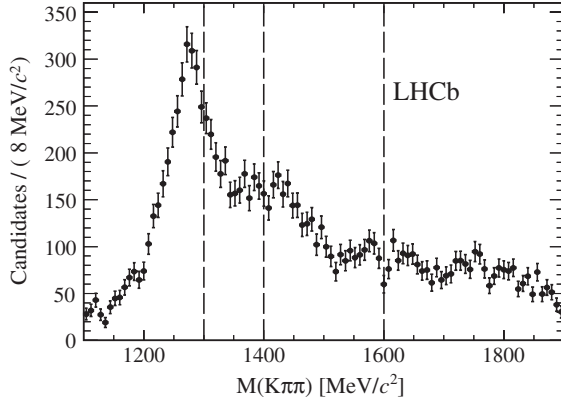


FIG. 2. Background-subtracted $K^+\pi^-\pi^+$ mass distribution of the $B^+ \rightarrow K^+\pi^-\pi^+\gamma$ signal. The four intervals of interest, separated by dashed lines, are shown.

$K^+\pi^-\pi^+$ mass spectrum. The up-down asymmetry is thus studied inclusively in four intervals of $K^+\pi^-\pi^+$ mass. The $[1.4, 1.6]$ GeV/c^2 interval, studied in Ref. [7], includes the $K_1(1400)^+$, $K_2^*(1430)^+$ and $K^*(1410)^+$ resonances with small contributions from the upper tail of the $K_1(1270)^+$. At the time of the writing of Ref. [7], the $K_1(1400)^+$ was believed to be the dominant 1^+ resonance, so the $K_1(1270)^+$ was not considered. However, subsequent experimental results [21] demonstrated that the $K_1(1270)^+$ is more prominent than the $K_1(1400)^+$; hence, the $[1.1, 1.3]$ GeV/c^2 interval is also studied here. The $[1.3, 1.4]$ GeV/c^2 mass interval, which contains the overlap region between the two K_1 resonances, and the $[1.6, 1.9]$ GeV/c^2 high mass interval, which includes spin-2 and spin-3 resonances, are also considered.

In each of the four $K^+\pi^-\pi^+$ mass intervals, a simultaneous fit to the B -candidate mass spectra in bins of the photon angle is performed in order to determine the background-subtracted angular distribution; the previously described PDF is used to model the mass spectrum in each bin, with all of the fit parameters being shared except for the yields. Since the sign of the photon polarization depends on the sign of the electric charge of the B candidate, the angular variable $\cos\hat{\theta} \equiv \text{charge}(B)\cos\theta$ is used. The resulting background-subtracted $\cos\hat{\theta}$ distribution, corrected for the selection acceptance and normalized to the inverse of the bin width, is fit with a fourth-order polynomial function normalized to unit area,

$$f(\cos\hat{\theta}; c_0 = 0.5, c_1, c_2, c_3, c_4) = \sum_{i=0}^4 c_i L_i(\cos\hat{\theta}), \quad (3)$$

where $L_i(x)$ is the Legendre polynomial of order i and c_i is the corresponding coefficient. Using Eqs. (1) and (3) the up-down asymmetry defined in Eq. (2) can be expressed as

$$\mathcal{A}_{\text{ud}} = c_1 - \frac{c_3}{4}. \quad (4)$$

As a cross-check, the up-down asymmetry in each mass interval is also determined with a counting method, rather than an angular fit, as well as considering separately the B^+ and B^- candidates. All these checks yield compatible results.

The results obtained from a χ^2 fit of the normalized binned angular distribution, performed taking into account the full covariance matrix of the bin contents and all of the systematic uncertainties, are summarized in Table I. These systematic uncertainties account for the effect of choosing a different fit model, the impact of the limited size of the simulated samples on the fixed parameters, and the possibility of some events migrating from a bin to its neighbor because of the detector resolution, which gives the dominant contribution. The systematic uncertainty associated with the fit model is determined by performing the mass fit using several alternative PDFs, while the other two are estimated with simulated pseudoexperiments. Such uncertainties, despite being of the same size as the statistical uncertainty, do not substantially affect the fit results since they are strongly correlated across all angular bins.

The fitted distributions in the four $K^+\pi^-\pi^+$ mass intervals of interest are shown in Fig. 3. In order to illustrate the effect of the up-down asymmetry, the results of another fit imposing $c_1 = c_3 = 0$, hence forbidding the terms that carry the λ_γ dependence, are overlaid for comparison.

The combined significance of the observed up-down asymmetries is determined from a χ^2 test where the null hypothesis is defined as $\lambda_\gamma = 0$, implying that the up-down asymmetry is expected to be zero in each mass interval. The corresponding χ^2 distribution has 4 degrees of freedom, and the observed value corresponds to a p value of 1.7×10^{-7} . This translates into a 5.2σ significance for nonzero up-down asymmetry. Up-down asymmetries can be computed also for an alternative definition of the photon

TABLE I. Legendre coefficients obtained from fits to the normalized background-subtracted $\cos\hat{\theta}$ distribution in the four $K^+\pi^-\pi^+$ mass intervals of interest. The up-down asymmetries are obtained from Eq. (4). The quoted uncertainties contain statistical and systematic contributions. The $K^+\pi^-\pi^+$ mass ranges are indicated in GeV/c^2 and all the parameters are expressed in units of 10^{-2} . The covariance matrices are given in Ref. [22].

	[1.1,1.3]	[1.3,1.4]	[1.4,1.6]	[1.6,1.9]
c_1	6.3 ± 1.7	5.4 ± 2.0	4.3 ± 1.9	-4.6 ± 1.8
c_2	31.6 ± 2.2	27.0 ± 2.6	43.1 ± 2.3	28.0 ± 2.3
c_3	-2.1 ± 2.6	2.0 ± 3.1	-5.2 ± 2.8	-0.6 ± 2.7
c_4	3.0 ± 3.0	6.8 ± 3.6	8.1 ± 3.1	-6.2 ± 3.2
\mathcal{A}_{ud}	6.9 ± 1.7	4.9 ± 2.0	5.6 ± 1.8	-4.5 ± 1.9

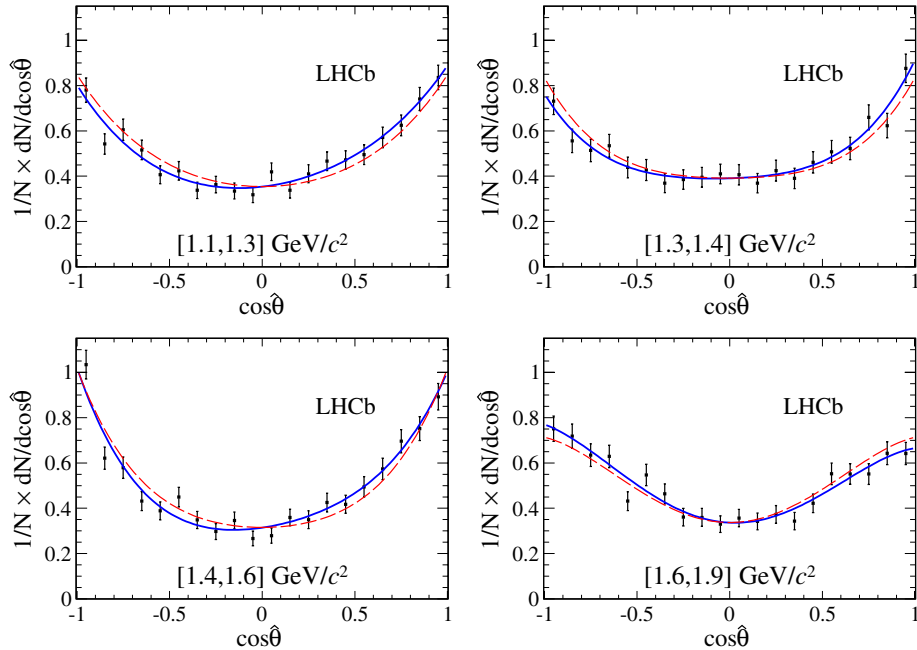


FIG. 3 (color online). Distributions of $\cos \hat{\theta}$ for $B^+ \rightarrow K^+ \pi^- \pi^+ \gamma$ signal in four intervals of $K^+ \pi^- \pi^+$ mass. The solid blue (dashed red) curves are the result of fits allowing all (only even) Legendre components up to the fourth power.

angle, obtained using the normal $\vec{p}_{\pi^-} \times \vec{p}_{\pi^+}$, instead of $\vec{p}_{\pi,\text{slow}} \times \vec{p}_{\pi,\text{fast}}$. The obtained values, along with the relative fit coefficients, are listed in Table II.

To summarize, a study of the inclusive flavor-changing neutral current radiative $B^+ \rightarrow K^+ \pi^- \pi^+ \gamma$ decay, with the $K^+ \pi^- \pi^+$ mass in the $[1.1, 1.9]$ GeV/c^2 range, is performed on a data sample corresponding to an integrated luminosity of 3 fb^{-1} collected in $p p$ collisions at 7 and 8 TeV center-of-mass energies by the LHCb detector. A total of 13876 ± 153 signal events is observed. The shape of the angular distribution of the photon with respect to the plane defined by the three final-state hadrons in their rest frame is determined in four intervals of interest in the $K^+ \pi^- \pi^+$ mass spectrum. The up-down asymmetry, which is proportional to the photon polarization, is measured for the first

TABLE II. Legendre coefficients obtained from fits to the normalized background-subtracted $\cos \hat{\theta}$ distribution, using the alternative normal $\vec{p}_{\pi^-} \times \vec{p}_{\pi^+}$ for defining the direction of the photon, in the four $K^+ \pi^- \pi^+$ mass intervals of interest. The up-down asymmetries are obtained from Eq. (4). The quoted uncertainties contain statistical and systematic contributions. The $K^+ \pi^- \pi^+$ mass ranges are indicated in GeV/c^2 and all the parameters are expressed in units of 10^{-2} . The covariance matrices are given in Ref. [22].

	$[1.1, 1.3]$	$[1.3, 1.4]$	$[1.4, 1.6]$	$[1.6, 1.9]$
c'_1	-0.9 ± 1.7	7.4 ± 2.0	5.3 ± 1.9	-3.4 ± 1.8
c'_2	31.6 ± 2.2	27.4 ± 2.6	43.6 ± 2.3	27.8 ± 2.3
c'_3	0.8 ± 2.6	0.8 ± 3.1	-4.4 ± 2.8	2.3 ± 2.7
c'_4	3.4 ± 3.0	7.0 ± 3.6	8.0 ± 3.1	-6.6 ± 3.2
A'_{ud}	-1.1 ± 1.7	7.2 ± 2.0	6.4 ± 1.8	-3.9 ± 1.9

time for each of these $K^+ \pi^- \pi^+$ mass intervals. The first observation of a parity-violating photon polarization different from zero at the 5.2σ significance level in $b \rightarrow s \gamma$ transitions is reported. The shape of the photon angular distribution in each bin, as well as the values for the up-down asymmetry, may be used, if theoretical predictions become available, to determine for the first time a value for the photon polarization, and thus constrain the effects of physics beyond the SM in the $b \rightarrow s \gamma$ sector.

We express our gratitude to our colleagues in the CERN accelerator departments for the excellent performance of the LHC. We thank the technical and administrative staff at the LHCb institutes. We acknowledge support from CERN and from the national agencies: CAPES, CNPq, FAPERJ, and FINEP (Brazil); NSFC (China); CNRS/IN2P3 and Region Auvergne (France); BMBF, DFG, HGF, and MPG (Germany); SFI (Ireland); INFN (Italy); FOM and NWO (The Netherlands); SCSR (Poland); MEN/IFA (Romania); MinES, Rosatom, RFBR, and NRC “Kurchatov Institute” (Russia); MinECo, XuntaGal, and GENCAT (Spain); SNSF and SER (Switzerland); NAS Ukraine (Ukraine); STFC (United Kingdom); NSF (USA). We also acknowledge the support received from the ERC under FP7. The Tier1 computing centres are supported by IN2P3 (France), KIT and BMBF (Germany), INFN (Italy), NWO and SURF (Netherlands), PIC (Spain), GridPP (United Kingdom). We are indebted towards the communities behind the multiple open source software packages we depend on. We are also thankful for the computing resources and the access to software R&D tools provided by Yandex LLC (Russia).

- [1] J. Beringer *et al.* (Particle Data Group), *Phys. Rev. D* **86**, 010001 (2012), and 2013 partial update for the 2014 edition.
- [2] J. C. Pati and A. Salam, *Phys. Rev. D* **10**, 275 (1974); **11** 703 (1975); R. Mohapatra and J. C. Pati, *Phys. Rev. D* **11**, 2558 (1975); R. N. Mohapatra and J. C. Pati, *Phys. Rev. D* **11**, 566 (1975); G. Senjanovic and R. N. Mohapatra, *Phys. Rev. D* **12**, 1502 (1975); G. Senjanovic, *Nucl. Phys.* **B153**, 334 (1979); R. N. Mohapatra and G. Senjanovic, *Phys. Rev. D* **23**, 165 (1981); C. Lim and T. Inami, *Prog. Theor. Phys.* **67**, 1569 (1982); L. Everett, S. Rigolin, G. L. Kane, L.-T. Wang, and T. T. Wang, *J. High Energy Phys.* **01** (2002) 022.
- [3] D. Atwood, M. Gronau, and A. Soni, *Phys. Rev. Lett.* **79**, 185 (1997).
- [4] S. Nishida *et al.* (Belle Collaboration), *Phys. Rev. Lett.* **89**, 231801 (2002).
- [5] B. Aubert *et al.* (BaBar Collaboration), *Phys. Rev. Lett.* **98**, 211804 (2007).
- [6] C. S. Wu, E. Ambler, R. W. Hayward, D. D. Hoppes, and R. P. Hudson, *Phys. Rev.* **105**, 1413 (1957).
- [7] M. Gronau and D. Pirjol, *Phys. Rev. D* **66**, 054008 (2002).
- [8] E. Kou, A. Le Yaouanc, and A. Tayduganov, *Phys. Rev. D* **83**, 094007 (2011).
- [9] A. A. Alves, Jr. *et al.* (LHCb Collaboration), *JINST* **3**, S08005 (2008).
- [10] T. Sjöstrand, S. Mrenna, and P. Skands, *J. High Energy Phys.* **05** (2006) 026; *Comput. Phys. Commun.* **178**, 852 (2008).
- [11] I. Belyaev *et al.*, *Nuclear Science Symposium Conference Record (NSS/MIC)*, (IEEE, Bellingham, WA, 2010), p. 1155.
- [12] D. J. Lange, *Nucl. Instrum. Methods Phys. Res., Sect. A* **462**, 152 (2001).
- [13] P. Golonka and Z. Was, *Eur. Phys. J. C* **45**, 97 (2006).
- [14] J. Allison *et al.* (Geant4 Collaboration), *IEEE Trans. Nucl. Sci.* **53**, 270 (2006); S. Agostinelli *et al.*, (Geant4 Collaboration), *Nucl. Instrum. Methods Phys. Res., Sect. A* **506**, 250 (2003).
- [15] M. Clemencic, G. Corti, S. Easo, C. R. Jones, S. Miglioranzi, M. Pappagallo, and P. Robbe, *J. Phys. Conf. Ser.* **331**, 032023 (2011).
- [16] L. Breiman, J. H. Friedman, R. A. Olshen, and C. J. Stone, *Classification and Regression Trees* (Wadsworth International Group, Belmont, CA, 1984).
- [17] R. E. Schapire and Y. Freund, *J. Comput. Syst. Sci.* **55**, 119 (1997).
- [18] T. Skwarnicki, Ph.D thesis, Institute of Nuclear Physics, 1986 [DESY F31-86-02, Appendix E].
- [19] H. Albrecht *et al.* (ARGUS Collaboration), *Phys. Lett. B* **241**, 278 (1990).
- [20] M. Pivk and F. R. Le Diberder, *Nucl. Instrum. Methods Phys. Res., Sect. A* **555**, 356 (2005).
- [21] H. Yang *et al.* (Belle Collaboration), *Phys. Rev. Lett.* **94**, 111802 (2005).
- [22] See Supplemental Material at <http://link.aps.org/supplemental/10.1103/PhysRevLett.112.161801> for details.

R. Aaij,⁴¹ B. Adeva,³⁷ M. Adinolfi,⁴⁶ A. Affolder,⁵² Z. Ajaltouni,⁵ J. Albrecht,⁹ F. Alessio,³⁸ M. Alexander,⁵¹ S. Ali,⁴¹ G. Alkhazov,³⁰ P. Alvarez Cartelle,³⁷ A. A. Alves Jr.,²⁵ S. Amato,² S. Amerio,²² Y. Amhis,⁷ L. Anderlini,^{17,a} J. Anderson,⁴⁰ R. Andreassen,⁵⁷ M. Andreotti,^{16,b} J. E. Andrews,⁵⁸ R. B. Appleby,⁵⁴ O. Aquines Gutierrez,¹⁰ F. Archilli,³⁸ A. Artamonov,³⁵ M. Artuso,⁵⁹ E. Aslanides,⁶ G. Auriemma,^{25,c} M. Baalouch,⁵ S. Bachmann,¹¹ J. J. Back,⁴⁸ A. Badalov,³⁶ V. Balagura,³¹ W. Baldini,¹⁶ R. J. Barlow,⁵⁴ C. Barschel,³⁹ S. Barsuk,⁷ W. Barter,⁴⁷ V. Batozskaya,²⁸ T. Bauer,⁴¹ A. Bay,³⁹ J. Beddow,⁵¹ F. Bedeschi,²³ I. Bediaga,¹ S. Belogurov,³¹ K. Belous,³⁵ I. Belyaev,³¹ E. Ben-Haim,⁸ G. Bencivenni,¹⁸ S. Benson,⁵⁰ J. Benton,⁴⁶ A. Berezhnoy,³² R. Bernet,⁴⁰ M.-O. Bettler,⁴⁷ M. van Beuzekom,⁴¹ A. Bien,¹¹ S. Bifani,⁴⁵ T. Bird,⁵⁴ A. Bizzeti,^{17,d} P. M. Bjørnstad,⁵⁴ T. Blake,⁴⁸ F. Blanc,³⁹ J. Blouw,¹⁰ S. Blusk,⁵⁹ V. Bocci,²⁵ A. Bondar,³⁴ N. Bondar,³⁰ W. Bonivento,^{15,38} S. Borghi,⁵⁴ A. Borgia,⁵⁹ M. Borsato,⁷ T. J. V. Bowcock,⁵² E. Bowen,⁴⁰ C. Bozzi,¹⁶ T. Brambach,⁹ J. van den Brand,⁴² J. Bressieux,³⁹ D. Brett,⁵⁴ M. Britsch,¹⁰ T. Britton,⁵⁹ N. H. Brook,⁴⁶ H. Brown,⁵² A. Bursche,⁴⁰ G. Busetto,^{22,e} J. Buytaert,³⁸ S. Cadeddu,¹⁵ R. Calabrese,^{16,b} O. Callot,⁷ M. Calvi,^{20,f} M. Calvo Gomez,^{36,g} A. Camboni,³⁶ P. Campana,^{18,38} D. Campora Perez,³⁸ F. Caponio,²¹ A. Carbone,^{14,h} G. Carboni,^{24,i} R. Cardinale,^{19,j} A. Cardini,¹⁵ H. Carranza-Mejia,⁵⁰ L. Carson,⁵⁰ K. Carvalho Akiba,² G. Casse,⁵² L. Cassina,²⁰ L. Castillo Garcia,³⁸ M. Cattaneo,³⁸ C. Cauet,⁹ R. Cenci,⁵⁸ M. Charles,⁸ P. Charpentier,³⁸ S.-F. Cheung,⁵⁵ N. Chiapolini,⁴⁰ M. Chrzaszcz,^{40,26} K. Ciba,³⁸ X. Cid Vidal,³⁸ G. Ciezarek,⁵³ P. E. L. Clarke,⁵⁰ M. Clemencic,³⁸ H. V. Cliff,⁴⁷ J. Closier,³⁸ C. Coca,²⁹ V. Coco,³⁸ J. Cogan,⁶ E. Cogneras,⁵ P. Collins,³⁸ A. Comerma-Montells,³⁶ A. Contu,^{15,38} A. Cook,⁴⁶ M. Coombes,⁴⁶ S. Coquereau,⁸ G. Corti,³⁸ I. Counts,⁵⁶ B. Couturier,³⁸ G. A. Cowan,⁵⁰ D. C. Craik,⁴⁸ M. Cruz Torres,⁶⁰ S. Cunliffe,⁵³ R. Currie,⁵⁰ C. D'Ambrosio,³⁸ J. Dalseno,⁴⁶ P. David,⁸ P. N. Y. David,⁴¹ A. Davis,⁵⁷ I. De Bonis,⁴ K. De Bruyn,⁴¹ S. De Capua,⁵⁴ M. De Cian,¹¹ J. M. De Miranda,¹ L. De Paula,² W. De Silva,⁵⁷ P. De Simone,¹⁸ D. Decamp,⁴ M. Deckenhoff,⁹ L. Del Buono,⁸ N. Déléage,⁴ D. Derkach,⁵⁵ O. Deschamps,⁵ F. Dettori,⁴² A. Di Canto,¹¹ H. Dijkstra,³⁸ S. Donleavy,⁵² F. Dordei,¹¹ M. Dorigo,³⁹ P. Dorosz,^{26,k} A. Dosil Suárez,³⁷ D. Dossett,⁴⁸ A. Dovbnya,⁴³ F. Dupertuis,³⁹ P. Durante,³⁸ R. Dzhelyadin,³⁵ A. Dziurda,²⁶ A. Dzyuba,³⁰ S. Easo,⁴⁹ U. Egede,⁵³ V. Egorychev,³¹ S. Eidelman,³⁴ S. Eisenhardt,⁵⁰ U. Eitschberger,⁹ R. Ekelhof,⁹ L. Eklund,^{51,38} I. El Rifai,⁵ C. Elsasser,⁴⁰ S. Esen,¹¹ A. Falabella,^{16,b} C. Färber,¹¹ C. Farinelli,⁴¹ S. Farry,⁵² D. Ferguson,⁵⁰ V. Fernandez Albor,³⁷ F. Ferreira Rodrigues,¹ M. Ferro-Luzzi,³⁸ S. Filippov,³³ M. Fiore,^{16,b} M. Fiorini,^{16,b} C. Fitzpatrick,³⁸ M. Fontana,¹⁰

- F. Fontanelli,^{19,j} R. Forty,³⁸ O. Francisco,² M. Frank,³⁸ C. Frei,³⁸ M. Frosini,^{17,38,a} J. Fu,²¹ E. Furfaro,^{24,i} A. Gallas Torreira,³⁷ D. Galli,^{14,h} S. Gambetta,^{19,j} M. Gandelman,² P. Gandini,⁵⁹ Y. Gao,³ J. Garofoli,⁵⁹ J. Garra Tico,⁴⁷ L. Garrido,³⁶ C. Gaspar,³⁸ R. Gauld,⁵⁵ L. Gavardi,⁹ E. Gersabeck,¹¹ M. Gersabeck,⁵⁴ T. Gershon,⁴⁸ P. Ghez,⁴ A. Gianelle,²² S. Giani,³⁹ V. Gibson,⁴⁷ L. Giubega,²⁹ V. V. Gligorov,³⁸ C. Göbel,⁶⁰ D. Golubkov,³¹ A. Golutvin,^{53,31,38} A. Gomes,^{1,l} H. Gordon,³⁸ M. Grabalosa Gándara,⁵ R. Graciani Diaz,³⁶ L. A. Granado Cardoso,³⁸ E. Graugés,³⁶ G. Graziani,¹⁷ A. Grecu,²⁹ E. Greening,⁵⁵ S. Gregson,⁴⁷ P. Griffith,⁴⁵ L. Grillo,¹¹ O. Grünberg,⁶¹ B. Gui,⁵⁹ E. Gushchin,³³ Y. Guz,^{35,38} T. Gys,³⁸ C. Hadjivasiliou,⁵⁹ G. Haefeli,³⁹ C. Haen,³⁸ T. W. Hafkenscheid,⁶⁴ S. C. Haines,⁴⁷ S. Hall,⁵³ B. Hamilton,⁵⁸ T. Hampson,⁴⁶ S. Hansmann-Menzemer,¹¹ N. Harnew,⁵⁵ S. T. Harnew,⁴⁶ J. Harrison,⁵⁴ T. Hartmann,⁶¹ J. He,³⁸ T. Head,³⁸ V. Heijne,⁴¹ K. Hennessy,⁵² P. Henrard,⁵ L. Henry,⁸ J. A. Hernando Morata,³⁷ E. van Herwijnen,³⁸ M. Heß,⁶¹ A. Hicheur,¹ D. Hill,⁵⁵ M. Hoballah,⁵ C. Hombach,⁵⁴ W. Hulsbergen,⁴¹ P. Hunt,⁵⁵ N. Hussain,⁵⁵ D. Hutchcroft,⁵² D. Hynds,⁵¹ M. Idzik,²⁷ P. Ilten,⁵⁶ R. Jacobsson,³⁸ A. Jaeger,¹¹ E. Jans,⁴¹ P. Jaton,³⁹ A. Jawahery,⁵⁸ F. Jing,³ M. John,⁵⁵ D. Johnson,⁵⁵ C. R. Jones,⁴⁷ C. Joram,³⁸ B. Jost,³⁸ N. Jurik,⁵⁹ M. Kaballo,⁹ S. Kandybei,⁴³ W. Kango,⁶ M. Karacson,³⁸ T. M. Karbach,³⁸ M. Kelsey,⁵⁹ I. R. Kenyon,⁴⁵ T. Ketel,⁴² B. Khanji,²⁰ C. Khurewathanakul,³⁹ S. Klaver,⁵⁴ O. Kochebina,⁷ I. Komarov,³⁹ R. F. Koopman,⁴² P. Koppenburg,⁴¹ M. Korolev,³² A. Kozlinskiy,⁴¹ L. Kravchuk,³³ K. Kreplin,¹¹ M. Kreps,⁴⁸ G. Krocker,¹¹ P. Krokovny,³⁴ F. Kruse,⁹ M. Kucharczyk,^{20,26,38,f} V. Kudryavtsev,³⁴ K. Kurek,²⁸ T. Kvaratskheliya,^{31,38} V. N. La Thi,³⁹ D. Lacarrere,³⁸ G. Lafferty,⁵⁴ A. Lai,¹⁵ D. Lambert,⁵⁰ R. W. Lambert,⁴² E. Lanciotti,³⁸ G. Lanfranchi,¹⁸ C. Langenbruch,³⁸ B. Langhans,³⁸ T. Latham,⁴⁸ C. Lazzeroni,⁴⁵ R. Le Gac,⁶ J. van Leerdam,⁴¹ J.-P. Lees,⁴ R. Lefèvre,⁵ A. Leflat,³² J. Lefrançois,⁷ S. Leo,²³ O. Leroy,⁶ T. Lesiak,²⁶ B. Leverington,¹¹ Y. Li,³ M. Liles,⁵² R. Lindner,³⁸ C. Linn,³⁸ F. Lionetto,⁴⁰ B. Liu,¹⁵ G. Liu,³⁸ S. Lohn,³⁸ I. Longstaff,⁵¹ J. H. Lopes,² N. Lopez-March,³⁹ P. Lowdon,⁴⁰ H. Lu,³ D. Lucchesi,^{22,e} H. Luo,⁵⁰ E. Luppi,^{16,b} O. Lupton,⁵⁵ F. Machefert,⁷ I. V. Machikhiliyan,³¹ F. Maciuc,²⁹ O. Maev,^{30,38} S. Malde,⁵⁵ G. Manca,^{15,m} G. Mancinelli,⁶ M. Manzali,^{16,b} J. Maratas,⁵ U. Marconi,¹⁴ C. Marin Benito,³⁶ P. Marino,^{23,n} R. Märki,³⁹ J. Marks,¹¹ G. Martellotti,²⁵ A. Martens,⁸ A. Martín Sánchez,⁷ M. Martinelli,⁴¹ D. Martinez Santos,⁴² F. Martinez Vidal,⁶³ D. Martins Tostes,² A. Massafferri,¹ R. Matev,³⁸ Z. Mathe,³⁸ C. Matteuzzi,²⁰ A. Mazurov,^{16,38,b} M. McCann,⁵³ J. McCarthy,⁴⁵ A. McNab,⁵⁴ R. McNulty,¹² B. McSkelly,⁵² B. Meadows,^{57,55} F. Meier,⁹ M. Meissner,¹¹ M. Merk,⁴¹ D. A. Milanes,⁸ M.-N. Minard,⁴ J. Molina Rodriguez,⁶⁰ S. Monteil,⁵ D. Moran,⁵⁴ M. Morandin,²² P. Morawski,²⁶ A. Mordà,⁶ M. J. Morello,^{23,n} R. Mountain,⁵⁹ F. Muheim,⁵⁰ K. Müller,⁴⁰ R. Muresan,²⁹ B. Muryn,²⁷ B. Muster,³⁹ P. Naik,⁴⁶ T. Nakada,³⁹ R. Nandakumar,⁴⁹ I. Nasteva,¹ M. Needham,⁵⁰ N. Neri,²¹ S. Neubert,³⁸ N. Neufeld,³⁸ A. D. Nguyen,³⁹ T. D. Nguyen,³⁹ C. Nguyen-Mau,^{39,o} M. Nicol,⁷ V. Niess,⁵ R. Niet,⁹ N. Nikitin,³² T. Nikodem,¹¹ A. Novoselov,³⁵ A. Oblakowska-Mucha,²⁷ V. Obraztsov,³⁵ S. Oggero,⁴¹ S. Ogilvy,⁵¹ O. Okhrimenko,⁴⁴ R. Oldeman,^{15,m} G. Onderwater,⁶⁴ M. Orlandea,²⁹ J. M. Otalora Goicochea,² P. Owen,⁵³ A. Oyanguren,³⁶ B. K. Pal,⁵⁹ A. Palano,^{13,p} F. Palombo,^{21,q} M. Palutan,¹⁸ J. Panman,³⁸ A. Papanestis,^{49,38} M. Pappagallo,⁵¹ L. Pappalardo,¹⁶ C. Parkes,⁵⁴ C. J. Parkinson,⁹ G. Passaleva,¹⁷ G. D. Patel,⁵² M. Patel,⁵³ C. Patrignani,^{19,j} C. Pavel-Nicorescu,²⁹ A. Pazos Alvarez,³⁷ A. Pearce,⁵⁴ A. Pellegrino,⁴¹ M. Pepe Altarelli,³⁸ S. Perazzini,^{14,h} E. Perez Trigo,³⁷ P. Perret,⁵ M. Perrin-Terrin,⁶ L. Pescatore,⁴⁵ E. Pesen,⁶⁵ G. Pessina,²⁰ K. Petridis,⁵³ A. Petrolini,^{19,j} E. Picatoste Olloqui,³⁶ B. Pietrzyk,⁴ T. Pilär,⁴⁸ D. Pinci,²⁵ A. Pistone,¹⁹ S. Playfer,⁵⁰ M. Plo Casasus,³⁷ F. Polci,⁸ A. Poluektov,^{48,34} E. Polycarpo,² A. Popov,³⁵ D. Popov,¹⁰ B. Popovici,²⁹ C. Potterat,³⁶ A. Powell,⁵⁵ J. Prisciandaro,³⁹ A. Pritchard,⁵² C. Prouve,⁴⁶ V. Pugatch,⁴⁴ A. Puig Navarro,³⁹ G. Punzi,^{23,r} W. Qian,⁴ B. Rachwal,²⁶ J. H. Rademacker,⁴⁶ B. Rakotomaramanana,³⁹ M. Rama,¹⁸ M. S. Rangel,² I. Raniuk,⁴³ N. Rauschmayr,³⁸ G. Raven,⁴² S. Reichert,⁵⁴ M. M. Reid,⁴⁸ A. C. dos Reis,¹ S. Ricciardi,⁴⁹ A. Richards,⁵³ K. Rinnert,⁵² V. Rives Molina,³⁶ D. A. Roa Romero,⁵ P. Robbe,⁷ D. A. Roberts,⁵⁸ A. B. Rodrigues,¹ E. Rodrigues,⁵⁴ P. Rodriguez Perez,³⁷ S. Roiser,³⁸ V. Romanovsky,³⁵ A. Romero Vidal,³⁷ M. Rotondo,²² J. Rouvinet,³⁹ T. Ruf,³⁸ F. Ruffini,²³ H. Ruiz,³⁶ P. Ruiz Valls,³⁶ G. Sabatino,^{25,i} J. J. Saborido Silva,³⁷ N. Sagidova,³⁰ P. Sail,⁵¹ B. Saitta,^{15,m} V. Salustino Guimaraes,² B. Sanmartin Sedes,³⁷ R. Santacesaria,²⁵ C. Santamarina Rios,³⁷ E. Santovetti,^{24,i} M. Sapunov,⁶ A. Sarti,¹⁸ C. Satriano,^{25,c} A. Satta,²⁴ M. Savrie,^{16,b} D. Savrina,^{31,32} M. Schiller,⁴² H. Schindler,³⁸ M. Schlupp,⁹ M. Schmelling,¹⁰ B. Schmidt,³⁸ O. Schneider,³⁹ A. Schopper,³⁸ M.-H. Schune,⁷ R. Schwemmer,³⁸ B. Sciascia,¹⁸ A. Sciubba,²⁵ M. Seco,³⁷ A. Semennikov,³¹ K. Senderowska,²⁷ I. Sepp,⁵³ N. Serra,⁴⁰ J. Serrano,⁶ P. Seyfert,¹¹ M. Shapkin,³⁵ I. Shapoval,^{16,43,b} Y. Shcheglov,³⁰ T. Shears,⁵² L. Shekhtman,³⁴ O. Shevchenko,⁴³ V. Shevchenko,⁶² A. Shires,⁹ R. Silva Coutinho,⁴⁸ G. Simi,²² M. Sirendi,⁴⁷ N. Skidmore,⁴⁶ T. Skwarnicki,⁵⁹ N. A. Smith,⁵² E. Smith,^{55,49} E. Smith,⁵³ J. Smith,⁴⁷ M. Smith,⁵⁴ H. Snoek,⁴¹ M. D. Sokoloff,⁵⁷ F. J. P. Soler,⁵¹ F. Soomro,³⁹ D. Souza,⁴⁶ B. Souza De Paula,² B. Spaan,⁹ A. Sparkes,⁵⁰ F. Spinella,²³ P. Spradlin,⁵¹ F. Stagni,³⁸ S. Stahl,¹¹ O. Steinkamp,⁴⁰ S. Stevenson,⁵⁵ S. Stoica,²⁹ S. Stone,⁵⁹ B. Storaci,⁴⁰ S. Stracka,^{23,38} M. Straticiuc,²⁹

U. Straumann,⁴⁰ R. Stroili,²² V. K. Subbiah,³⁸ L. Sun,⁵⁷ W. Sutcliffe,⁵³ S. Swientek,⁹ V. Syropoulos,⁴² M. Szczekowski,²⁸ P. Szczypka,^{39,38} D. Szilard,² T. Szumlak,²⁷ S. T'Jampens,⁴ M. Teklishyn,⁷ G. Tellarini,^{16,b} E. Teodorescu,²⁹ F. Teubert,³⁸ C. Thomas,⁵⁵ E. Thomas,³⁸ J. van Tilburg,¹¹ V. Tisserand,⁴ M. Tobin,³⁹ S. Tolk,⁴² L. Tomassetti,^{16,b} D. Tonelli,³⁸ S. Topp-Joergensen,⁵⁵ N. Torr,⁵⁵ E. Tournefier,^{4,53} S. Tourneur,³⁹ M. T. Tran,³⁹ M. Tresch,⁴⁰ A. Tsaregorodtsev,⁶ P. Tsopelas,⁴¹ N. Tuning,⁴¹ M. Ubeda Garcia,³⁸ A. Ukleja,²⁸ A. Ustyuzhanin,⁶² U. Uwer,¹¹ V. Vagnoni,¹⁴ G. Valenti,¹⁴ A. Vallier,⁷ R. Vazquez Gomez,¹⁸ P. Vazquez Regueiro,³⁷ C. Vázquez Sierra,³⁷ S. Vecchi,¹⁶ J. J. Velthuis,⁴⁶ M. Veltre,^{17,s} G. Veneziano,^{39,t} M. Vesterinen,¹¹ B. Viaud,⁷ D. Vieira,² X. Vilasis-Cardona,^{36,g} A. Vollhardt,⁴⁰ D. Volyanskyy,¹⁰ D. Voong,⁴⁶ A. Vorobyev,³⁰ V. Vorobyev,³⁴ C. Voß,⁶¹ H. Voss,¹⁰ J. A. de Vries,⁴¹ R. Waldi,⁶¹ C. Wallace,⁴⁸ R. Wallace,¹² S. Wandernoth,¹¹ J. Wang,⁵⁹ D. R. Ward,⁴⁷ N. K. Watson,⁴⁵ A. D. Webber,⁵⁴ D. Websdale,⁵³ M. Whitehead,⁴⁸ J. Wicht,³⁸ J. Wiechczynski,²⁶ D. Wiedner,¹¹ G. Wilkinson,⁵⁵ M. P. Williams,^{48,49} M. Williams,⁵⁶ F. F. Wilson,⁴⁹ J. Wimberley,⁵⁸ J. Wishahi,⁹ W. Wislicki,²⁸ M. Witek,²⁶ G. Wormser,⁷ S. A. Wotton,⁴⁷ S. Wright,⁴⁷ S. Wu,³ K. Wyllie,³⁸ Y. Xie,^{50,38} Z. Xing,⁵⁹ Z. Yang,³ X. Yuan,³ O. Yushchenko,³⁵ M. Zangoli,¹⁴ M. Zavertyaev,^{10,t} F. Zhang,³ L. Zhang,⁵⁹ W. C. Zhang,¹² Y. Zhang,³ A. Zhelezov,¹¹ A. Zhokhov,³¹ L. Zhong³ and A. Zvyagin³⁸

(LHCb Collaboration)

¹Centro Brasileiro de Pesquisas Físicas (CBPF), Rio de Janeiro, Brazil

²Universidade Federal do Rio de Janeiro (UFRJ), Rio de Janeiro, Brazil

³Center for High Energy Physics, Tsinghua University, Beijing, China

⁴LAPP, Université de Savoie, CNRS/IN2P3, Annecy-Le-Vieux, France

⁵Clermont Université, Université Blaise Pascal, CNRS/IN2P3, LPC, Clermont-Ferrand, France

⁶CPPM, Aix-Marseille Université, CNRS/IN2P3, Marseille, France

⁷LAL, Université Paris-Sud, CNRS/IN2P3, Orsay, France

⁸LPNHE, Université Pierre et Marie Curie, Université Paris Diderot, CNRS/IN2P3 Paris, France

⁹Fakultät Physik, Technische Universität Dortmund, Dortmund, Germany

¹⁰Max-Planck-Institut für Kernphysik (MPIK), Heidelberg, Germany

¹¹Physikalisches Institut, Ruprecht-Karls-Universität Heidelberg, Heidelberg, Germany

¹²School of Physics, University College Dublin, Dublin, Ireland

¹³Sezione INFN di Bari, Bari, Italy

¹⁴Sezione INFN di Bologna, Bologna, Italy

¹⁵Sezione INFN di Cagliari, Cagliari, Italy

¹⁶Sezione INFN di Ferrara, Ferrara, Italy

¹⁷Sezione INFN di Firenze, Firenze, Italy

¹⁸Laboratori Nazionali dell'INFN di Frascati, Frascati, Italy

¹⁹Sezione INFN di Genova, Genova, Italy

²⁰Sezione INFN di Milano Bicocca, Milano, Italy

²¹Sezione INFN di Milano, Milano, Italy

²²Sezione INFN di Padova, Padova, Italy

²³Sezione INFN di Pisa, Pisa, Italy

²⁴Sezione INFN di Roma Tor Vergata, Roma, Italy

²⁵Sezione INFN di Roma La Sapienza, Roma, Italy

²⁶Henryk Niewodniczanski Institute of Nuclear Physics Polish Academy of Sciences, Kraków, Poland

²⁷Faculty of Physics and Applied Computer Science, AGH—University of Science and Technology, Kraków, Poland

²⁸National Center for Nuclear Research (NCBJ), Warsaw, Poland

²⁹Horia Hulubei National Institute of Physics and Nuclear Engineering, Bucharest-Magurele, Romania

³⁰Petersburg Nuclear Physics Institute (PNPI), Gatchina, Russia

³¹Institute of Theoretical and Experimental Physics (ITEP), Moscow, Russia

³²Institute of Nuclear Physics, Moscow State University (SINP MSU), Moscow, Russia

³³Institute for Nuclear Research of the Russian Academy of Sciences (INR RAN), Moscow, Russia

³⁴Budker Institute of Nuclear Physics (SB RAS) and Novosibirsk State University, Novosibirsk, Russia

³⁵Institute for High Energy Physics (IHEP), Protvino, Russia

³⁶Universitat de Barcelona, Barcelona, Spain

³⁷Universidad de Santiago de Compostela, Santiago de Compostela, Spain

³⁸European Organization for Nuclear Research (CERN), Geneva, Switzerland

³⁹Ecole Polytechnique Fédérale de Lausanne (EPFL), Lausanne, Switzerland

⁴⁰Physik-Institut, Universität Zürich, Zürich, Switzerland

⁴¹Nikhef National Institute for Subatomic Physics, Amsterdam, The Netherlands

⁴²Nikhef National Institute for Subatomic Physics and VU University Amsterdam, Amsterdam, The Netherlands⁴³NSC Kharkiv Institute of Physics and Technology (NSC KIPT), Kharkiv, Ukraine⁴⁴Institute for Nuclear Research of the National Academy of Sciences (KINR), Kyiv, Ukraine⁴⁵University of Birmingham, Birmingham, United Kingdom⁴⁶H.H. Wills Physics Laboratory, University of Bristol, Bristol, United Kingdom⁴⁷Cavendish Laboratory, University of Cambridge, Cambridge, United Kingdom⁴⁸Department of Physics, University of Warwick, Coventry, United Kingdom⁴⁹STFC Rutherford Appleton Laboratory, Didcot, United Kingdom⁵⁰School of Physics and Astronomy, University of Edinburgh, Edinburgh, United Kingdom⁵¹School of Physics and Astronomy, University of Glasgow, Glasgow, United Kingdom⁵²Oliver Lodge Laboratory, University of Liverpool, Liverpool, United Kingdom⁵³Imperial College London, London, United Kingdom⁵⁴School of Physics and Astronomy, University of Manchester, Manchester, United Kingdom⁵⁵Department of Physics, University of Oxford, Oxford, United Kingdom⁵⁶Massachusetts Institute of Technology, Cambridge, Massachusetts, USA⁵⁷University of Cincinnati, Cincinnati, Ohio, USA⁵⁸University of Maryland, College Park, Maryland, USA⁵⁹Syracuse University, Syracuse, New York, USA⁶⁰Pontifícia Universidade Católica do Rio de Janeiro (PUC-Rio), Rio de Janeiro, Brazil

(associated with Universidade Federal do Rio de Janeiro (UFRJ), Rio de Janeiro, Brazil)

⁶¹Institut für Physik, Universität Rostock, Rostock, Germany

(associated with Physikalisches Institut, Ruprecht-Karls-Universität Heidelberg, Heidelberg, Germany)

⁶²National Research Centre Kurchatov Institute, Moscow, Russia

(associated with Institute of Theoretical and Experimental Physics (ITEP), Moscow, Russia)

⁶³Instituto de Física Corpuscular (IFIC), Universitat de València-CSIC, Valencia, Spain

(associated with Universitat de Barcelona, Barcelona, Spain)

⁶⁴KVI—University of Groningen, Groningen, The Netherlands

(associated with Nikhef National Institute for Subatomic Physics, Amsterdam, The Netherlands)

⁶⁵Celal Bayar University, Manisa, Turkey

(associated with European Organization for Nuclear Research (CERN), Geneva, Switzerland)

^aAlso at Università di Firenze, Firenze, Italy.^bAlso at Università di Ferrara, Ferrara, Italy.^cAlso at Università della Basilicata, Potenza, Italy.^dAlso at Università di Modena e Reggio Emilia, Modena, Italy.^eAlso at Università di Padova, Padova, Italy.^fAlso at Università di Milano Bicocca, Milano, Italy.^gAlso at LIFAELS, La Salle, Universitat Ramon Llull, Barcelona, Spain.^hAlso at Università di Bologna, Bologna, Italy.ⁱAlso at Università di Roma Tor Vergata, Roma, Italy.^jAlso at Università di Genova, Genova, Italy.^kAlso at AGH - University of Science and Technology, Faculty of Computer Science, Electronics and Telecommunications, Kraków, Poland.^lAlso at Universidade Federal do Triângulo Mineiro (UFTM), Uberaba-MG, Brazil.^mAlso at Università di Cagliari, Cagliari, Italy.ⁿAlso at Scuola Normale Superiore, Pisa, Italy.^oAlso at Hanoi University of Science, Hanoi, Vietnam.^pAlso at Università di Bari, Bari, Italy.^qAlso at Università degli Studi di Milano, Milano, Italy.^rAlso at Università di Pisa, Pisa, Italy.^sAlso at Università di Urbino, Urbino, Italy.^tAlso at P.N. Lebedev Physical Institute, Russian Academy of Science (LPI RAS), Moscow, Russia.[†]Corresponding author.giovanni.veneziano@cern.ch